Chemistry & Biology
Article

Measuring In Vivo Protein Half-Life

Karolina Bojkowska,[1] Francesca Santoni de Sio,[1] Isabelle Barde,[1] Sandra Offner,[1] Sonia Verp,[1] Christian Heinis,[2] Kai Johnsson,[2,*] and Didier Trono[1,*]
[1]School of Life Sciences, "Frontiers-in-Genetics" National Program
[2]Institute of Chemical Sciences and Engineering
Ecole Polytechnique Fédérale de Lausanne, CH-1015 Lausanne, Switzerland
*Correspondence: kai.johnsson@epfl.ch (K.J.), didier.trono@epfl.ch (D.T.)
DOI 10.1016/j.chembiol.2011.03.014

SUMMARY

Protein turnover critically influences many biological functions, yet methods have been lacking to assess this parameter in vivo. Here, we demonstrate how chemical labeling of SNAP-tag fusion proteins can be exploited to measure the half-life of resident intracellular and extracellular proteins in living mice. First, we demonstrate that SNAP-tag substrates have wide bioavailability in mice and can be used for the specific in vivo labeling of SNAP-tag fusion proteins. We then apply near-infrared probes to perform noninvasive imaging of in vivo-labeled tumors. Finally, we use SNAP-mediated chemical pulse-chase labeling to perform measurement of the in vivo half-life of different extra- and intracellular proteins. These results open broad perspectives for studying protein function in living animals.

INTRODUCTION

The stability and turnover of proteins in live cells is a carefully controlled parameter that affects numerous biological functions, which cell cycle, transcriptional control, or DNA damage response are just a few examples of (Hershko and Ciechanover, 1998, Lakin and Jackson, 1999). Additionally, half-life of specific proteins is altered in pathological situations such as viral infections (Mangasarian et al., 1997), neurodegenerative disorders (Shin et al., 2011), or cancer (Hershko and Ciechanover, 1998). A better understanding of degradation rates of specific proteins in different conditions would facilitate drug development for various human diseases (Bedford et al., 2011).

Traditionally, metabolic pulse-chase with isotopically labeled amino acids has been used for decades to monitor the stability of specific proteins in tissue culture (Dickson and Mendenhall, 2004), and a method of global profiling has recently been described that allows the scale-up of such analyses to thousands of proteins at a time (Yen et al., 2008). Isotopically labeled amino acids have recently been used to measure protein turnover in vivo by mass spectrometry, and this technique was applied to determine the synthesis and degradation rates of β-amyloid in human patients of Alzheimer'sdisease (Bateman et al., 2006; Mawuenyega et al., 2010). While an exciting development, this approach has a number of limitations. First, the infusion of an isotopically labeled amino acid and its subsequent washout is much slower in vivo than in tissue culture. The resulting lower temporal resolution restricts the use of the approach to the study of proteins characterized by rather long half-lives. Furthermore, pulse-chase labeling in vivo or in vitro does not permit to distinguish between proteins present in different cellular compartments, such as the plasma membrane and the secretory pathway. The latter point is of critical importance when the stability of membrane proteins is investigated. In light of the importance of protein turnover in biological processes (Ciechanover, 2005; Hershko and Ciechanover, 1998), it can thus be concluded that there is an urgent need for alternative and complementary approaches to measure this parameter in vivo.

A powerful approach to characterize the properties of a protein of interest is based on its expression as a fusion protein with an appropriate tag. Fluorescent proteins (FPs) have been the most widely exploited tags for studies of localization and function of their fusion partners (Giepmans et al., 2006). Recently, photoactivated variants of FPs have been generated that permit monitoring protein turnover in cell culture (Fuchs et al., 2010). However, the necessary photo-activation cannot easily be performed in the depth of a living animal. As an alternative, various chemical labeling techniques have been developed (Fernandez-Suarez and Ting, 2008; Marks and Nolan, 2006). Chemical labeling has been shown to be a versatile approach for studying a range of protein properties, including protein stability, activity, trafficking, and interactions with other biomolecules (Fernandez-Suarez and Ting, 2008; Marks and Nolan, 2006; Tsukiji et al., 2009). Chemical labeling provides a choice of probes each tailored for a specific application. For example, synthetic fluorophores are available that are ideally suited for either characterizing protein-protein interactions by Förster resonance energy transfer measurements or for noninvasive imaging in living animals (Maurel et al., 2008; Tannous et al., 2006). Additionally, chemical labeling permits the labeling of proteins at selected time points to differentiate between different generations of a given protein (so-called pulse-chase labeling experiments; Gaietta et al., 2002). This has been exploited to measure the half-life of fusion proteins in cell culture and to visualize the formation of biological structures (Gaietta et al., 2002; Jansen et al., 2007; Vivero-Pol et al., 2005) and potentially might also permit to study protein half-life in living animals.

One self-labeling tag that appears particularly well suited for measuring in vivo protein half-life through chemical labeling is the so-called SNAP-tag. SNAP-tag is a mutant of human O^6-alkylguanine-DNA alkyltransferase (AGT) that permits

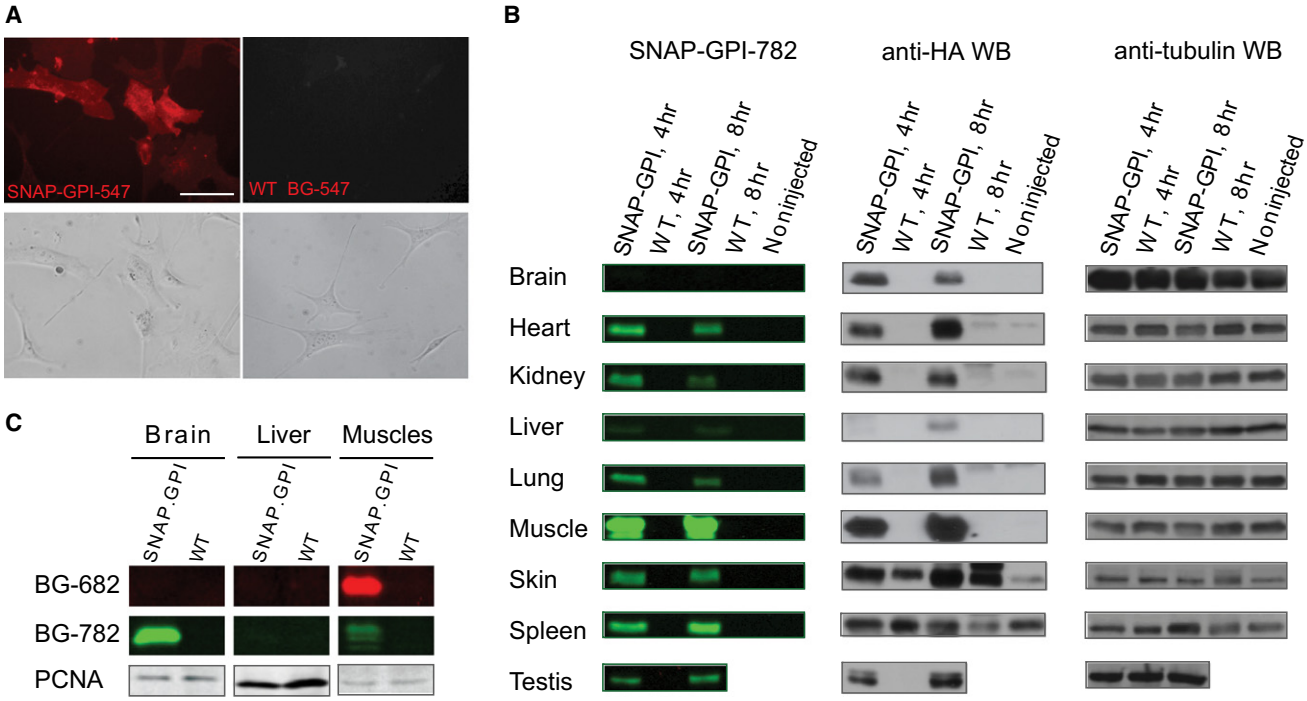

Figure 1. In Vivo Chemical Labeling of SNAP-GPI Transgenic Mice

(A) Phenotyping of SNAP-GPI transgenic mice on primary ear fibroblasts. In vitro cultured primary fibroblasts from SNAP-GPI (left) or WT (right) mice were labeled with BG-547 and imaged under a wide-field fluorescence microscope. Top and bottom represent fluorescent and phase contrast images, respectively. Scale bar is 100 μm.

(B) Assessing in vivo protein labeling with BG-782 of SNAP-GPI transgenic mice by SDS-PAGE of protein extracts and subsequent in-gel fluorescence scanning. Organs were harvested 4 and 8 hr after injection of BG-782. Wild-type mice injected with BG-782 or noninjected mice were used as controls. Left: fluorescent in-gel scan. Middle: HA-specific western blotting; in the skin and spleen of WT mice, a background band, that could come from cross-reactivity of the secondary anti-mouse IgG antibody with endogenous immunoglobulins present in the tissues, is present almost at the same apparent molecular weight as SNAP-GPI. Right: tubulin-specific western blotting as protein loading control.

(C) SNAP-GPI is highly expressed in the brain but not in the liver. Indicated mice were injected with BG-682 and organs were harvested after 4 hr. Tissues were labeled with BG-782 and protein extracts were resolved by SDS-PAGE.

See also Figure S1 and Table S1.

specific and irreversible labeling with O^6-benzylguanine (BG) derivatives carrying molecular probes (Gronemeyer et al., 2006; Keppler et al., 2003; Keppler et al., 2004). SNAP-tag has previously been used in cell culture for the pulse-chase labeling of intra- and extracellular proteins (Jansen et al., 2007; Keppler et al., 2004). It has also been demonstrated not to affect the function of a large number of fusion proteins (Hein et al., 2010; Jansen et al., 2007; Keppler et al., 2003, 2004; Klein et al., 2011; Maurel et al., 2008). BG was developed in the 1980s as a potent inhibitor of human AGT upregulated in various cancers and is used at very high doses in combination with chemotherapy in clinical trials for treatment of human tumors (Quinn et al., 2009). Pharmacology, metabolism and side effects of BG treatment have been extensively studied and described in mice, rats, and humans (Dolan et al., 1994; Sabharwal and Middleton, 2006). In these studies, no major side effects have been observed after in vivo administration of BG. Together, these properties make SNAP-tag an attractive candidate for measuring in vivo protein stability in living animals.

In the present study, we demonstrate that SNAP-tag can be used for in vivo imaging of fusion proteins in living mice and that the labeling is specific and efficient in most mouse organs. Moreover, we show that SNAP-tag can be used for in vivo pulse-chase experiments followed by an ex vivo protein analysis and determination of in vivo protein half-life in living organisms.

RESULTS

In Vivo Labeling of SNAP-Tag in Transgenic Mice

We first tested the efficiency of SNAP-tag labeling in living animals. We generated transgenic mice by perivitelline injection into a fertilized mouse oocyte of a lentivector expressing SNAP-tag fused to a GPI anchor (SNAP-GPI) from the ubiquitous CAG or ubiquitin C promoters. To verify that the transgene was correctly expressed on the cell surface, we phenotyped the mice by harvesting primary ear fibroblasts and labeling them in cell culture with BG-547 (further information concerning BG derivatives is provided in Table S1, available online). A cell surface-specific signal was detected in cells harvested from SNAP-GPI mice but not in the wild-type controls (Figure 1A). We then injected a series of BG derivatives into these animals and assessed the specific labeling of SNAP-GPI in various organs by SDS-PAGE of protein extracts followed by in-gel fluorescence scanning 4 and 8 hr after the probe injection. As illustrated

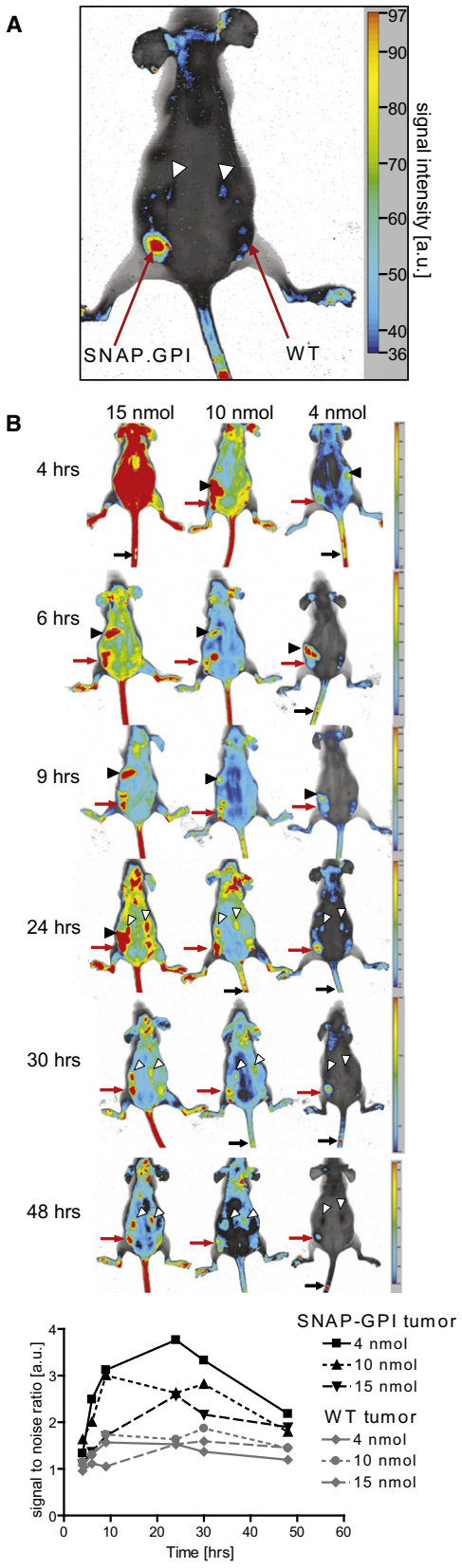

Figure 2. In Vivo Labeling and Noninvasive Imaging of SNAP-GPI-Expressing Tumors

(A) In vivo imaging of a nude mouse bearing TSA SNAP-GPI (left) and WT (right) tumors 24 hr after an intravenous injection of BG-782.

(B) In vivo labeling of tumor-bearing mice with different doses of BG derivatives. Top: Three nude mice bearing SNAP-GPI expressing tumor (left flank) or WT tumor (right flank) were injected with indicated doses of BG-782 and imaging was performed at the indicated time points. Red arrows indicate the SNAP-GPI tumor; black arrows indicate the injection site; black and white arrowheads indicate probe accumulated in the intestines and in kidneys, respectively. The brightness and contrast were optimized in later time points in order to visualize the signal. Bottom: Graph represents the ratio of signal from SNAP-GPI (black lines) and WT (gray lines) tumors to background of mouse tissues from experiment depicted in *B* for the indicated doses of BG-782.

for the BG-782 probe, specific labeling occurred in most of the organs examined (Figure 1B; Figure S1). The fluorescent signal was strong in muscles, heart, kidney, spleen, skin, lungs, and testis, while it was weaker in the liver, and hardly detectable in the brain. Similar results were obtained with other probes tested (Table S1; data not shown). SNAP-GPI expression in the various organs was analyzed in parallel by western blotting with an antibody against the HA-tag carried by the SNAP-tag fusion protein (Figure 1B). Strong expression was confirmed in most organs including the brain, but not in the liver. This indicated that the lack of live labeling in the liver stemmed from the very low expression of SNAP-GPI in this organ, while for its counterpart in the brain, it most likely resulted from a failure of the label to cross the blood-brain barrier. This was confirmed by harvesting organs from mice injected with BG-682, labeling them in vitro with BG-782 and analyzing the samples by SDS-PAGE (Figure 1C). BG itself is known to diffuse through the blood-brain barrier and inhibit the endogenous O^6-alkylguanine-DNA alkyltransferase (AGT) in mice (Kreklau et al., 2001). However, the probes used here carry significant modifications compared with the parental molecule, explaining their altered bioavailability. These results demonstrate that BG derivatives have wide bioavailability, permitting specific labeling of SNAP-fusion proteins in different mouse tissues.

Noninvasive Imaging of SNAP-GPI-Expressing Tumors in Living Mice

To further evaluate properties of the probes available for SNAP-tag labeling, we asked if in vivo-labeled SNAP-tag can be detected noninvasively by imaging techniques. Nude mice were implanted with murine breast carcinoma cells either engineered to express SNAP-GPI or left unmodified as a negative control. When the tumor reached 0.5 cm^3 in size, the infrared fluorescent probe BG-782 was injected intravenously and imaging was performed 24 hr later. As illustrated in Figure 2A, a fluorescent signal was detected from SNAP-GPI-expressing but not from WT control tumors. We then determined the settings that gave the best signal-to-noise ratio. Mice bearing SNAP-GPI tumors were injected with 4, 10, or 15 nmol of BG-782 per mouse and imaged at several time points (Figure 2B). A strong signal was detected in SNAP-expressing tumor tissue at each time point for all of doses tested. Early after probe injection, unspecific signal from unbound probe was present in the gut and liver, while at later time points, only an unspecific signal resulting from the probe was detected in kidneys. However, after the majority of

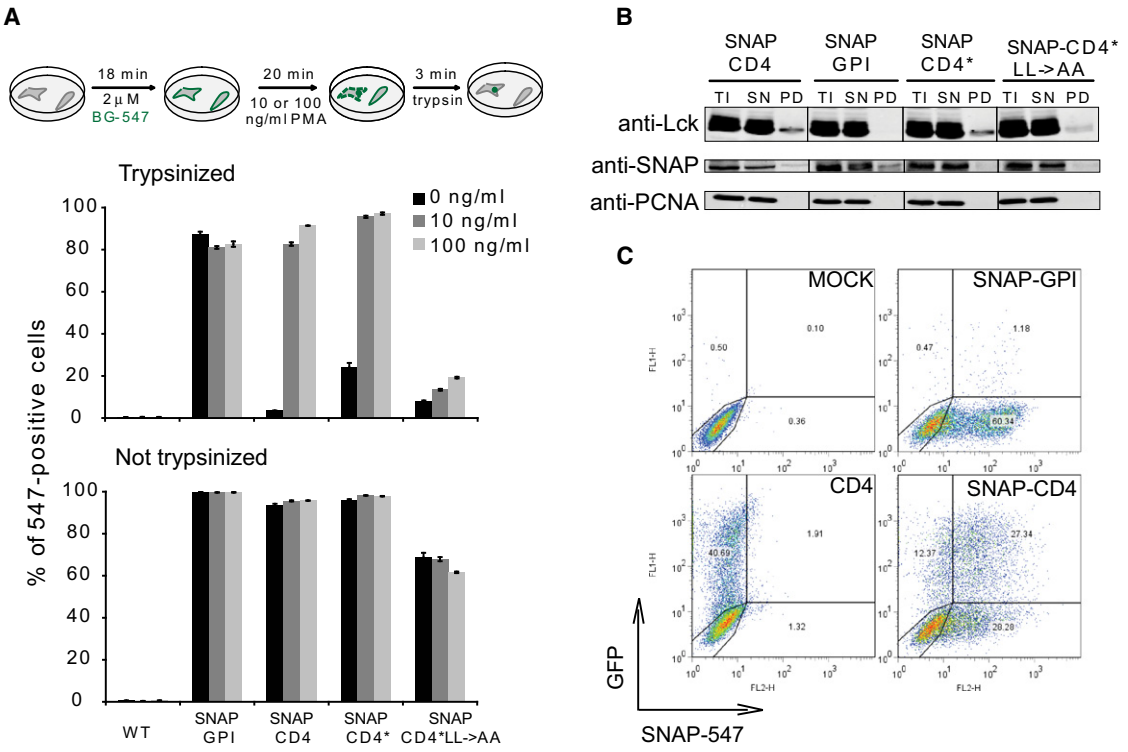

Figure 3. SNAP-CD4 Is Functional

(A) Upper panel: scheme of the experimental procedure. Jurkat cells expressing indicated SNAP fusion proteins first labeled with BG-547 were then blocked with BG and incubated with indicated doses of phorbol 12-myristate 13-acetate (PMA) at 37°C for 20 min. Middle and lower panel: Graphs show the percentage of BG-547 positive cells in the indicated samples trypsinized (middle) or not (lower), as assessed by flow cytometry. In SNAP-CD4* the extracellular domain of CD4 is replaced by SNAP. SNAP-CD4*LL- > AA is a double point mutant of CD4 ($Leu^{413,414}$- > $Ala^{413,414}$) resistant to PMA-induced endocytosis (Aiken et al., 1994). Error bars represent standard deviation.

(B) SNAP-CD4 but not SNAP-GPI recruits Lck. Protein extracts from Jurkat cells expressing indicated SNAP fusion proteins were incubated with agarose beads displaying BG. The immobilized proteins were then eluted and blotted with Lck- and SNAP-specific antibodies. TI-total input, SN-supernatant, PD-pull-down fraction.

(C) SNAP-CD4 can serve as a receptor for HIV-1. Flow cytometry analysis of 293T cells transfected with plasmids expressing SNAP-GPI, SNAP-CD4, or wt human CD4 and infected with a GFP-encoding lentiviral vector pseudotyped with lymphotropic HIV-1 envelope glycoprotein. Dot plots show GFP and SNAP-547 (red probe) expression 48 hr after labeling with BG-547.

See also Figure S2.

unbound probe was excreted from the system, strong signal above background was detected only in the SNAP-expressing tumor. Notably, after injection of 4 nmol of BG-782 the background from unbound probe was significantly lower than induced by higher doses, whereas SNAP-GPI tumor labeling was very efficient at all doses (Figure 2B). Thus, the lowest doses of BG-782 gave the best result, comparable to data previously obtained with infrared fluorescent proteins (Shu et al., 2009), and the best time for imaging was at 24 hr (Figure 2B). These results indicate that SNAP-tag fusion proteins in vivo-labeled with low doses of BG-782 can be noninvasively detected by means of fluorescence imaging.

Assessing the Possible Impact of SNAP-Tag on Fusion Protein Functionality and Stability In Vitro

We generated a SNAP-CD4 fusion protein (SNAP-CD4), in which the tag was placed downstream of the ER-targeting signal peptide of human CD4, and stably expressed this protein in human lymphoid Jurkat cells. We first tested the functionality of this molecule to ensure that SNAP-tag did not interfere with CD4 function. We performed an endocytosis assay in which cells expressing SNAP-CD4 were labeled with BG-547, washed and treated with various concentrations of phorbol-12-myristate-13-acetate (PMA) known to induce CD4 internalization (Pelchen-Matthews et al., 1991, 1993; Ruegg et al., 1992). Half of each sample was then trypsinized to digest extracellular proteins, including SNAP-CD4-782, and cells were analyzed by flow cytometry. In this assay, fluorescent signal observed after trypsynization results only from endocytosed SNAP-CD4-782. As shown in Figure 3A, we could verify that SNAP-CD4 underwent endocytosis upon cell activation with phorbol esters. Furthermore, using BG-coated magnetic beads, we could demonstrate that, as previously shown for the parental molecule CD4 (Aiken et al., 1994), SNAP-CD4 interacted with the Lck kinase (Figure 3B). Moreover, similarly to CD4 (Dalgleish et al., 1984), the SNAP-CD4 derivative served as an efficient receptor for HIV1 entry, as its expression was sufficient for infection of HEK293T cells with a lymphotropic, GFP-encoding lentiviral vector (Figure 3C).

After having determined that fusion with SNAP-tag does not perturb CD4 function, we determined the half-lives of SNAP-CD4 and SNAP-GPI in cultured Jurkat T cells. Jurkat T cells expressing these fusion proteins were labeled with 5 μM of cell-impermeable BG-782 and treated with 500 μM BG to block remaining unlabeled SNAP-tag. The cells were then harvested at sequential time points and the amount of labeled SNAP-tag was determined by in-gel fluorescence scanning of proteins resolved by SDS-PAGE (Figure 4A; Figure S3A). Comparable to previously published data for the rate of turnover of CD4 (Aiken et al., 1994; Pelchen-Matthews et al., 1991, 1993; Ruegg et al., 1992), the half-life of cell surface-labeled SNAP-CD4 was 5.2 hr, while that of SNAP-GPI was 3.8 hr. SNAP-CD4 was rapidly endocytosed and degraded upon PMA treatment, which reduced its postcell surface migration half-life to about 48 min (Figures 3A and 4A; Figure S3A) and increased its intracellular fraction from 10% to 80% (Figure 4B). These results are in agreement with previous studies focused on the effect of phorbol esters on rate of turnover of wild-type CD4 (Pelchen-Matthews et al., 1991, 1993; Ruegg et al., 1992), where PMA treatment of a lymphoid cell line SupT1 resulted in a decrease of post-cell surface migration half-life of CD4 to ~20 min. In the current study CD4 half-life is determined in yet another cell line, with use of lower doses of PMA (10 ng/ml compared to 100 ng/ml in Pelchen-Matthews et al., 1993). We believe that the slight differences in post-cell surface migration half-life between the two studies are due to the experimental conditions. In summary, these experiments thus established that SNAP-CD4 retains the function of wild-type CD4 and that its half-live can be readily determined through pulse-chase labeling in vitro.

As a further control, we verified that labeling of SNAP-tag did not lead to its ubiquitination and degradation in proteasome, as has been reported for parental AGT (Daniels et al., 2000; Xu-Welliver and Pegg, 2002). For this, we measured the in vitro ubiquitylation of SNAP-tag before and after its labeling (Figure S2). The results demonstrated that labeling triggered only minimal levels of ubiquitylation, with the modified protein representing at most 2.5% of its nonubiquitylated counterpart. These results are also in agreement with previously published data where pulse-chase labeling of SNAP-CENP-A was applied in living cells to follow the labeled fusion protein for more than two cell divisions and no degradation could be detected (Jansen et al., 2007).

In Vivo Determination of the Half-Life of a Cell Surface Protein

The subcutaneous implantation of the modified Jurkat cells in immunodeficient mice led to formation of tumors that were easily detectable by noninvasive fluorescence imaging after in vivo labeling of the surface fraction of SNAP-CD4 molecules with the cell-impermeable near-infrared probe BG-782 (Figure 5A). To demonstrate the feasibility of pulse-chase labeling experiments in vivo, we injected BG-782 (the pulse) in Rag2-γchain KO immunodeficient mice bearing subcutaneous Jurkat-derived tumors expressing SNAP-CD4, followed by a high dose of BG (the chase) (Figure 5B). One hour after the in vivo injection of BG, tumors were isolated and tissue homogenates incubated with BG-fluorescein. BG-fluorescein displays nonoverlapping excitation and emission spectra relative to BG-782 (Table S1), allowing a distinction of signals resulting from in vivo and in vitro-labeling reactions. No labeling of SNAP-CD4 with fluorescein could be detected whereas a strong fluorescein labeling was observed when the in vivo labeling steps were omitted (Figure 5B). These experiments demonstrate that chemical labeling of SNAP-tag lends itself to pulse-chase experiments in living animals and that both the pulse and the chase can be completed in 1 hr at most.

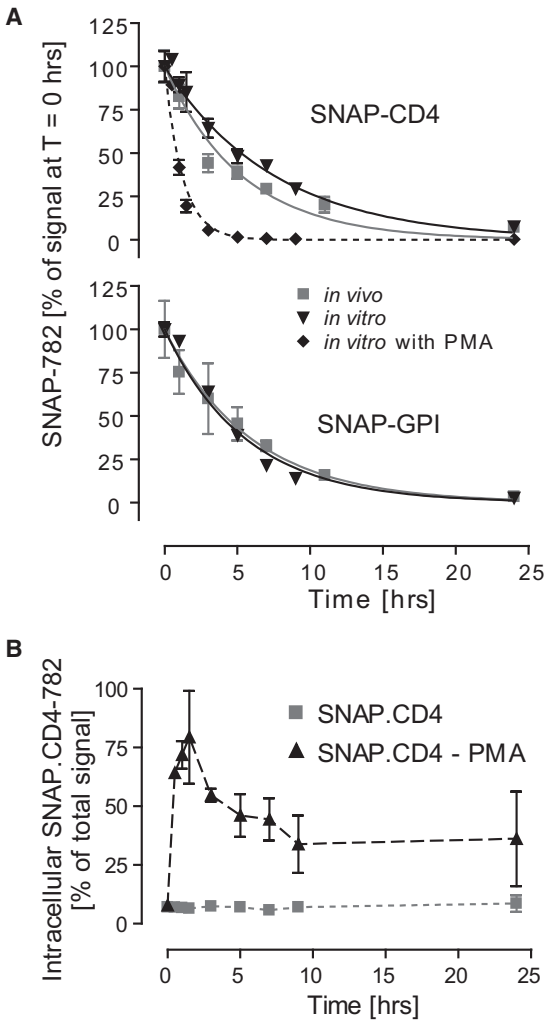

Figure 4. In Vitro and In Vivo Pulse-Chase of Extracellular SNAP-Fusion Proteins

Cells (n = 3–6 for SNAP-CD4; n = 7 for SNAP-GPI; average of two independent experiments) or mice (n = 4) bearing SNAP-tag expressing Jurkat tumors were pulse-labeled with BG-782, blocked with BG and samples were harvested at different time points.

(A) Quantification of fluorescent signal by SDS-PAGE gels of pulse-chase experiments of SNAP-CD4 (top) and SNAP-GPI (bottom) expressing cells. Data are fitted to a single exponential decay equation. Graphs show SNAP-782 signal at different time points after blocking as percentage of time 0 hr signal.

(B) SNAP-CD4 pool in the endosome. The graph shows quantification of fluorescent signal from protein extracts resolved by SDS-PAGE at different time points after blocking as a percentage of total fluorescent signal from cells without trypsinization.

See also Figure S3. Error bars represent SEM.

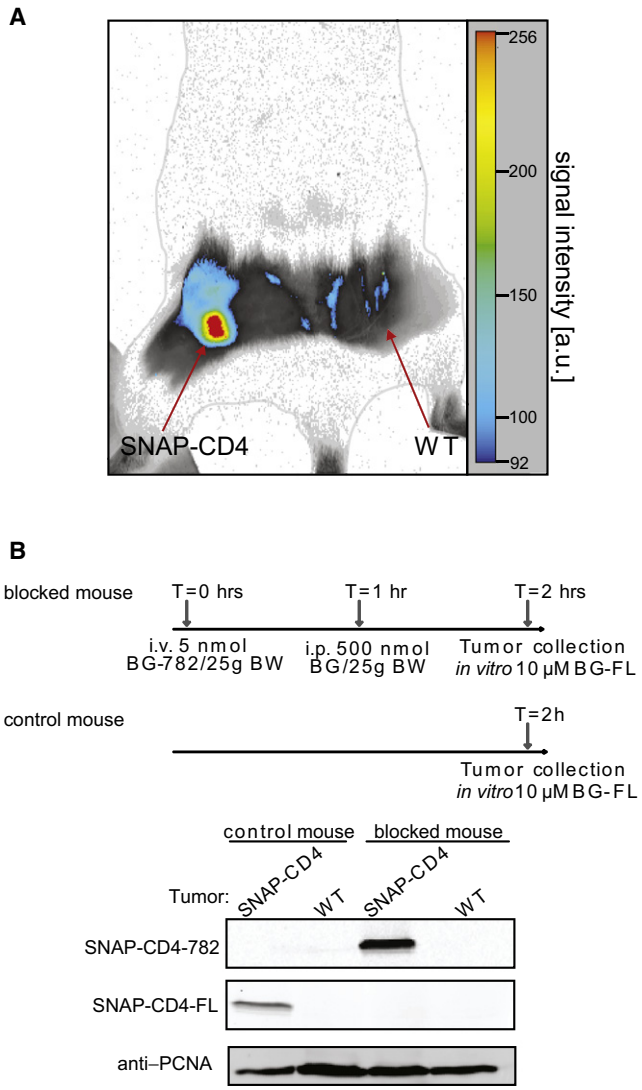

Figure 5. In Vivo Labeling of Mice Bearing SNAP-CD4-Expressing Jurkat T Cell-Derived Tumors

(A) In vivo imaging of a Rag2γ_cKO mouse bearing SNAP-CD4 (left) and WT (right) tumors 24 hr after an intravenous injection of BG-782 (200 pmol/g BW). Hair was removed prior to imaging.

(B) In vivo blocking of SNAP-CD4 with high-dose BG. Upper panels: scheme of the experimental procedure. Rag2γcKO mice bearing SNAP-CD4-expressing and control tumors were injected intravenously with 5 nmol/25 g BW of BG-782 (blocked mouse) or vehicle alone (control mouse). The labeled protein was chased with 500 nmol of BG per 25 g BW (blocked mouse). Tumor tissue was in vitro labeled with 10 μM BG-fluorescein. Lower panel: protein extracts were resolved by SDS-PAGE and examined by in-gel fluorescence scanning.

Rag2-γchain KO-immunodeficient mice bearing subcutaneous Jurkat-derived tumors expressing either SNAP-CD4 or SNAP-GPI were injected with BG-782 (pulse) and 1 hr later with a high dose of BG (chase). Protein extracts prepared from tumors harvested at sequential time points were then analyzed by SDS-PAGE and in-gel fluorescence scanning (Figure 4A; Figure S3B). Application of this chemical labeling technique allowed us to measure in vivo half-lives of SNAP-CD4 and SNAP-GPI, which were 3.7 and 4.1 hr, respectively. The accelerated turnover of SNAP-CD4 in living mice compared with cell culture could reflect increased levels of cellular activation in vivo, consistent with differences between the in vitro and in vivo models further emphasizing the importance of studying protein function in living organisms.

In Vivo Determination of the Half-Life of a Nuclear Protein

In the previous experiments, labeling was facilitated by extracellular expression of SNAP-tag fusion proteins. To test the generality of the in vivo pulse-chase labeling method, we then asked whether it could be applied to intracellular proteins. We fused SNAP-tag to murine KAP1 (Krüppel associated box (KRAB)-associated protein 1), an epigenetic master regulator (Sripathy et al., 2006; Figure 6). The resulting SNAP-KAP1 fusion protein was almost exclusively nuclear (Figure 6A), its expression was comparable with that of endogenous KAP1 in mouse embryonic fibroblasts (MEFs) (Figure 6B) and, similarly to its wild-type counterpart, SNAP-KAP1 was functional in a reporter assay based on tTR-KRAB (tetracycline repressor from *Escherichia coli* fused to KRAB domain)-mediated repression of GFP transcription (Figure 6C). We then determined that the half-life of SNAP-KAP1 in MEFs was 17.5 hr (Figure 7A; Figure S4A). In order to examine this latter parameter in vivo, we transplanted hematopoietic stem cells transduced ex vivo with a SNAP-KAP1 expressing lentiviral vector into lethally irradiated mice. We then pulsed the mice with the cell-permeable SNAP-tag substrate TMR-Star, blocked the labeling reaction with a high dose of BG, harvested spleens at different time points, and processed the samples through SDS-PAGE and in-gel fluorescence scanning (Figure 7B; Figure S4B). As observed for the BG-782 tested in transgenic and tumor bearing mice (Figures 1, 2, and 4), CP-TMR also diffused to spleen for SNAP-tag labeling. Using this approach, we determined that the in vivo half-life of SNAP-KAP1 in the spleen was 11 hr. The expression levels of the SNAP-KAP1 fusion protein observed in these experiments were lower than that of its endogenous KAP1 counterpart in the spleen and other organs (Figure S5; data not shown), demonstrating that our approach permits the analysis of intracellular SNAP-tag fusion proteins expressed at low concentrations.

DISCUSSION

Rate of protein turnover in live cells is an important and carefully controlled parameter affecting many cellular functions. The specific chemical labeling of fusion proteins with small fluorescent probes to measure protein half-life is a powerful alternative to metabolic pulse-chase labeling with radioactive amino acids but so far has only been applied in cell culture experiments. In this study, we demonstrate for the first time how chemical labeling of SNAP-tag fusion proteins can be utilized to measure protein in vivo half-life in animals. Importantly, these experiments describe a general method to characterize a previously inaccessible key property of proteins.

In vivo labeling of SNAP-GPI transgenic mice demonstrated that BG derivatives have wide bioavailability and label SNAP fusion proteins in most organs. The lack of labeling in the brain could be explained by a lack of blood-brain barrier crossing by BG derivatives, probably due to their increased molecular weight

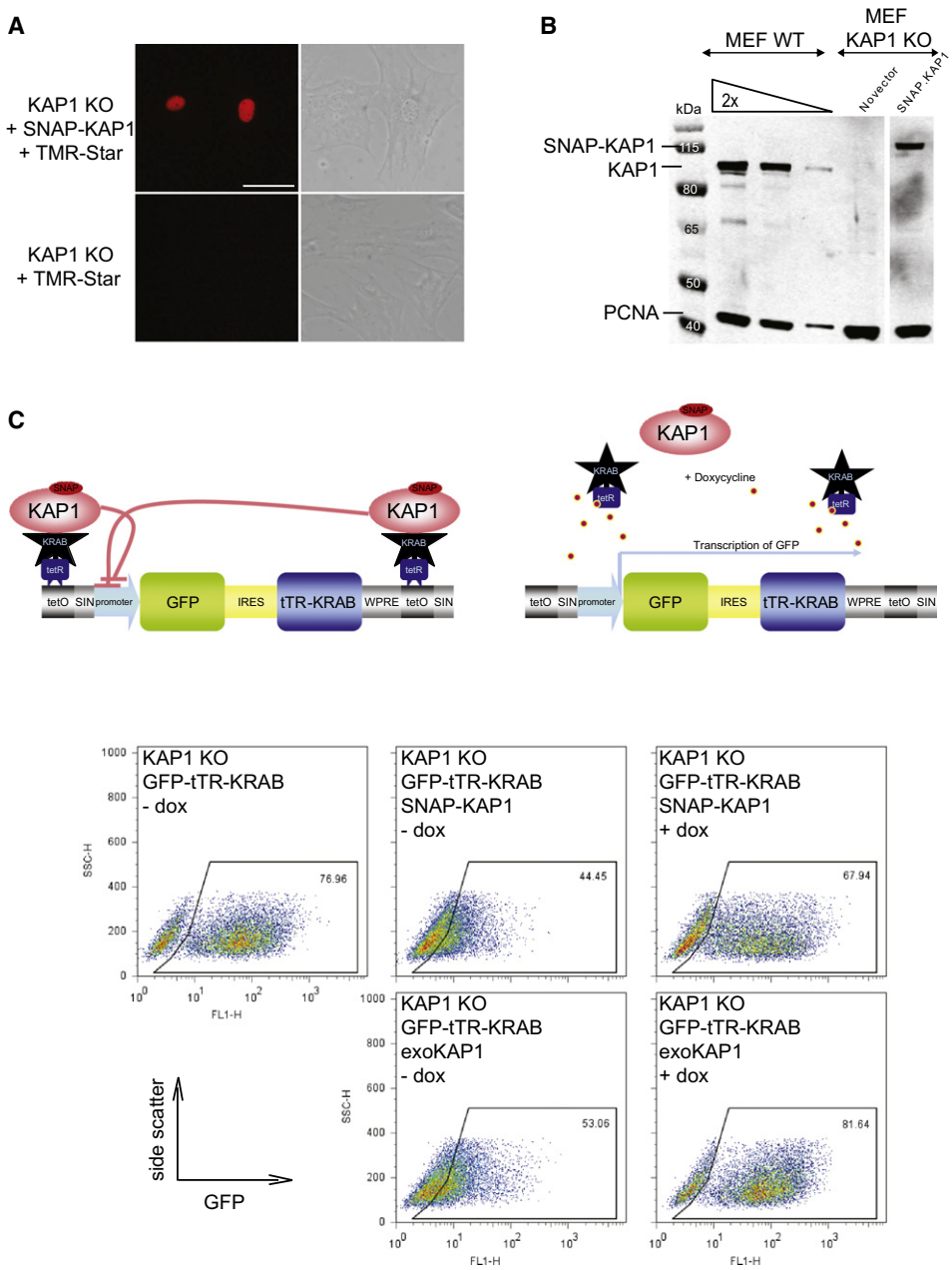

Figure 6. SNAP-KAP1 Is Functional

(A) SNAP-KAP1 expression in mouse embryonic fibroblasts (MEFs). MEFs KO for KAP1 were transduced with a lentivector encoding for SNAP-KAP1. Cells were labeled with 1 μM TMR-Star and washed prior to imaging. Scale bar is 100 μm.

(B) SNAP-KAP1 expression in MEFs is similar to that of endogenous KAP1 protein. Protein extracts from WT, KAP1 KO, and KAP1 KO MEFs transduced with SNAP-KAP1 encoding lentivector were resolved by SDS-PAGE transferred on a nitrocellulose membrane and blotted with anti-KAP1 and anti-PCNA antibodies.

(C) SNAP-KAP1 is a potent gene repressor. Upper cartoons: schematic of the vector encoding for GFP and tTR-KRAB repressor under the control of a doxycycline regulatable promoter used for KAP1 KO MEFs infection (left: in absence of doxycycline GFP is not transcribed; right: in presence of doxycycline GFP is transcribed). Lower panels: flow cytometry dot plots showing GFP expression in the presence (+ dox) and absence (- dox) of doxycycline of infected cells complemented with SNAP-KAP1 (top) or KAP1 alone (bottom).

and charge, as compared to the brain-reaching parent molecule BG (Kreklau et al., 2001). Indeed, other charged fluorescent probes have been shown to possess limited ability to penetrate the blood-brain barrier, which can in some cases be overcome by chemical modifications (Pham et al., 2005).

Chemical labeling of SNAP-tagged proteins have several advantages when compared with other available techniques. First, it shows high versatility and allows for exploiting a wide range of chemical moieties that can be utilized for labeling, in particular, when compared with the use of autofluorescent

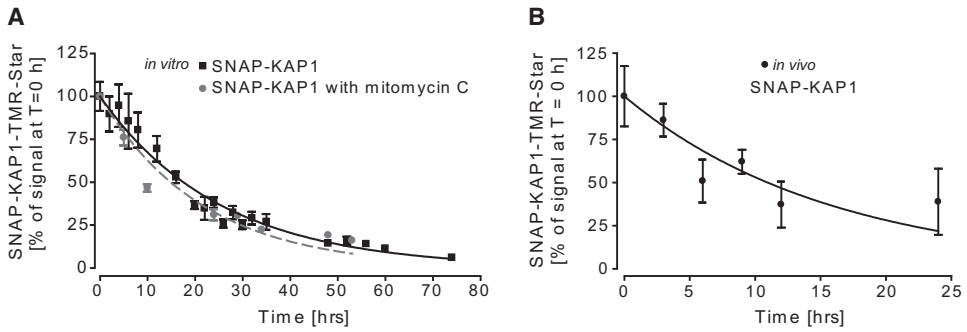

Figure 7. Pulse-Chase of SNAP-KAP1 in Mouse Embryonic Fibroblasts and in Mouse Spleen

(A) Graph shows average of fluorescent signal from two (SNAP-KAP1; n = 3-6) or one (SNAP-KAP1 upon mitomycin C treatment; n = 3) independent pulse-chase experiments.

(B) Graph shows the quantification of signal from SDS-PAGE gels from the in vivo pulse-chase experiment in SNAP-KAP1 expressing spleens of (n = 3–6) mice per time point. Signal at different time points is shown as percentage of time 0 hr signal. Data were fitted to a single exponential decay equation. Error bars represent SEM.

See also Figures S4 and S5.

proteins. In this study, we demonstrate that near-infrared fluorescent probes allow the noninvasive imaging of subcutaneous tumors upon in vivo labeling. It appears feasible that the method can be extended to probes endowed with different properties, for example, probes suitable for magnetic resonance imaging or positron emission tomography. However, our approach currently does not allow to measure protein turnover by noninvasive imaging, due to relatively slow pharmacokinetic clearance of the nonreacted probe. This limitation could potentially be overcome by the design of fluorogenic BG derivatives that become fluorescent only upon reaction with SNAP-tag. For example, fluorogenic substrates of matrix metalloproteinases have been successfully used for the imaging of these proteins in mice (Bremer et al., 2001).

A particularly attractive feature of chemical labeling over other protein tagging techniques is the control over the labeling time point. Additionally, it allows for use of different probes for labeling at different time points. Such pulse-chase labeling experiments are ideally suited for measuring protein half-life and to track biological structure formation. Accordingly, we demonstrate here that pulse-chase labeling of SNAP-fusion proteins represents a general method for the determination of in vivo protein half-life. Importantly, the described method can be applied to any protein amenable to expression as a fusion partner, whether cell-associated or secreted.

Our approach complements another approach to measure in vivo protein synthesis and clearance rates which was recently applied to determine β-amyloid turnover rates in humans afflicted with Alzheimer's disease (Bateman et al., 2006; Mawuenyega et al., 2010). This approach is based on injecting an isotopically labeled amino acid ($^{13}C_6$-leucine) followed by sample collection, immunoprecipitation of the protein of interest and high resolution tandem mass spectrometry (MS) to identify isotope-labeled species. The biggest conceptual advantage of this approach is that it permits the analysis of endogenous proteins. Nevertheless, it also has certain limitations. First, the infusion of an isotopically labeled amino acid and its subsequent washout is much slower in vivo than a corresponding experiment in tissue culture. To determine in vivo synthesis and clearance rates of β-amyloid, the authors performed a 9 hr continuous infusion of the isotope-labeled amino acid in patients (Bateman et al., 2006). Upon withdrawal of the isotope treatment, the plasma levels of $^{13}C_6$-leucine progressively decreased from 15% of total amino acid in plasma to 1% within 7 hr. By comparison, the time required for SNAP-tag in vivo labeling was 1 hr, whereas the chase with a high dose of BG was also completed within 1 hr. This proved important for the determination of the in vivo half-lives of proteins with relatively short half-lives (Figure 4). Additionally, isotope labeling does not distinguish between proteins present in different cellular compartments. In contrast, the use of BG derivatives with varying permeability permits to study the half-life of the extra- and intracellular populations of SNAP-tag fusions separately. For example, by using membrane impermeable probes the in vivo half-life of the extra-cellular population of CD4 could be determined. Both methods rely on quantification of the amount of isolated protein of interest at different time points and therefore require the sacrifice of numerous animals when proteins are investigated that cannot be isolated from body fluids.

In the cases studied here, SNAP-tag did not significantly affect the stability of its fusion partners and labeling itself did not affect this parameter either. In vivo measured protein half-lives were thus primarily determined by the stability of the parental molecules. It is impossible to predict and difficult to prove if a fusion protein faithfully copies the relevant properties of the corresponding wild-type protein (Johnsson and Johnsson, 2003). Experience accumulated in tissue culture with SNAP-tag indicates that it is no more problematic than any other commonly used tags. We also demonstrate that SNAP-tag fusion partners used in the current study retain the biological functions of their parental molecule (Figures 3 and 6). Nevertheless, it is crucial for the validity of our method that key protein functions such as localization and degradation rates of the fusion protein are investigated in vitro and compared with wild-type protein prior to proceeding with in vivo experiments.

In conclusion, our experiments show that chemical labeling of proteins is a versatile and valuable approach to study protein function in living animals. In particular, it permits the establishment of a general method to measure in vivo protein-half life.

The approach should therefore become an important tool for the characterization of mammalian proteins in their natural environment.

SIGNIFICANCE

Methods for measuring in vivo half-life of proteins are dearly needed both to pursue fundamental investigations and to develop and perform preclinical studies. Techniques based on chemical labeling have critically contributed to studies of protein function and stability in cell culture systems. Their application to the conduct of experiments in living organisms has not been extensive. Here, we demonstrate how chemical labeling can be used not only for labeling specific proteins in vivo and visualizing them by imaging methods, but also for determining their half-life in living mice. For this, we took advantage of SNAP-tag, a recently developed labeling method based on an engineered mutant of human O^6-alkylguanine-DNA alkyltransferase. Keys to the success of our approach are (1) the low toxicity of benzylguanine (BG) derivatives used for labeling, allowing for high in vivo probe concentrations; (2) the high specificity of the labeling of SNAP-tag, making it amenable for in vivo protein labeling in mice, (3) the fact that SNAP-tag is a relatively benign protein tag which generally does not affect the function of its fusion partner. By describing this new method for the evaluation of protein stability in vivo, our work opens broad perspectives for biological research.

EXPERIMENTAL PROCEDURES

Probes and Reagents

Benzylguanine derivatives and the SNAP-specific antibody were kindly provided by Covalys Biosciences (Switzerland) and New England Biolabs (US). Phorbol 12-myristate 13-acetate was obtained from Sigma-Aldrich (Switzerland). Lck-specific antibody was from United Biomedical (US); Anti-PCNA antibody was from EMD Biosciences (Germany); Anti-tubulin antibody was from Sigma-Aldrich (Switzerland), Anti-KAP1 antibody was from PTG labs, Manchester (UK), Anti-HA-HRP 3F10 antibody was from Roche (Switzerland).

Cell Culture, Vectors, and Transgenic Mice

Cells were cultured according to standard protocols as previously described (Barde et al., 2009; Maurice et al., 2002). Lentiviral vectors and transgenic mice were prepared according to standard protocols (Salmon and Trono, 2006; Lois et al., 2002). Details of plasmid sequences will be provided on demand. For in vitro labeling, cells expressing SNAP-tag were incubated with 1–2 μM BG derivatives for 5–15 min at 37°C and washed with cell culture medium before fixation with 1% formaldehyde (Sigma-Aldrich, Switzerland) in PBS for flow cytometry analysis or imaging. For mitomycin treatment, murine embryonic fibroblasts were incubated with 2 μg/ml of mitomycin C (Sigma-Aldrich) for 2.5 hr at 37°C 20 hr before the beginning of pulse-chase experiment.

In Vitro Pulse-Chase Experiments

Jurkat cells expressing SNAP fusion proteins were labeled for 15 min with 2 μM BG-547 (for flow cytometry) or BG-782 (for SDS-PAGE), washed, blocked with 500 μM BG and incubated with indicated doses of phorbol 12-myristate 13-acetate (PMA) at 37°C for 20 min. After extensive washing, half of the sample was trypsinized and cells were analyzed by flow cytometry or by SDS-PAGE followed by in-gel fluorescence scanning. In SNAP-CD4* the entire extracellular domain of CD4 is replaced by SNAP. SNAP-CD4*LL- > AA is a double point mutant of CD4 ($Leu^{413,414}$- > $Ala^{413,414}$) resistant to PMA-induced endocytosis (Aiken et al., 1994).

MEFs expressing SNAP-KAP1 were labeled with 1 μM of TMR-Star for 10 min, washed, and blocked with 500 μM BG. Samples were harvested at different time points for protein extraction and SDS-PAGE followed by fluorescence-in-gel scanning.

Lck Pull-Down Assay and Evaluation of SNAP-CD4 as a Receptor for HIV-1

Protein extracts from Jurkat cells expressing the indicated SNAP fusion proteins were incubated with agarose beads displaying BG (Covalys Biosciences, Switzerland). After extensive washing, the immobilized proteins were eluted, transferred on a nitrocellulose membrane and blotted with Lck- and SNAP-specific antibodies. 293T cells were transfected with 1 μg of plasmids expressing SNAP-GPI, SNAP-CD4, or wt human CD4. Twenty hours later, the cells were infected with a GFP-encoding lentiviral vector pseudotyped with lymphotropic HIV-1 envelope glycoprotein. After 48 hr, the cells were labeled with 2 μM BG-547, fixed, and analyzed by flow cytometry.

SDS-PAGE and Western Blotting

For SDS-PAGE in-gel fluorescence scanning and western blot analysis, protein extracts (20 μg for in vitro experiments or 100–150 μg for in vivo experiments) were resolved by SDS-PAGE, scanned on a Typhoon TRIO Variable Mode Imager (GE Healthcare, USA) or LI-COR Odyssey Imager (Germany) and then stained with Coomassie brilliant blue or transferred on a nitrocellulose membrane for western blotting with the indicated antibodies.

Mouse Tumor Models

Six-week-old female Crl:Nu(Ico)-Foxn1 nude (Charles Rivers, France) or Rag2γ_cKO mice (Taconic, USA) were injected subcutaneously with 10^6 TSA murine mammary carcinoma cells (kindly provided by Luigi Naldini) or 10^7 Jurkat T cells, respectively. Mice were examined daily and used for experiment when the tumor growth was visible, 2 or 4–5 weeks after TSA and Jurkat cell engraftment, respectively.

For in vivo imaging, at indicated time points after the indicated probe injection, mice were anaesthetized by inhalation of isolfluorane and imaged on LI-COR Odyssey Imager with use of the MousePOD accessory for in vivo imaging. Hair was removed from back of Rag2γ_cKO mice prior to imaging.

Hematopoietic Stem Cell Transplant Model

Murine HSCs harvested by flow cytometry sorting from bone marrow of donor CD45.1 males were transduced overnight with multiplicity of infection (MOI) of 250 of the RLL-hPGK-SNAP-HA-KAP1 vector and injected into lethally irradiated recipient CD45.2 females (14,000 HSC per mouse, together with 500,000 accessory total bone marrow cells). Mice were treated with antibiotic for 3 weeks and examined daily. Blood chimerism was estimated 5 weeks after the graft by staining peripheral blood mononuclear cells with antibodies against CD45.2 and CD45.1 and performing flow cytometry analysis. Chimerism was 30%–50%. Animals were used for in vivo pulse-chase 8–10 weeks after the HSC transplant.

In Vivo Labeling and Pulse-Chase Experiments

Labeling of transgenic mice was performed by intravenous injection of 120–200 pmol/g body weight (BW) of the indicated probes. Mice bearing SNAP-tag expressing Jurkat derived tumors were in vivo pulsed with 5 nmol BG-782/25 g BW and the unlabeled protein was chased with a 100 times higher dose of BG. Tumors were harvested at different time points after the labeling, tissue was incubated with 10 μM of BG-fluorescein to check for unlabeled SNAP (not shown), and the protein extracts were resolved by SDS-PAGE and analyzed by in-gel fluorescence scanning.

Mice, engrafted with HSCs transduced with SNAP-KAP1 vector, received an intravenous injection of 800 pmol of TMR-Star per gram of BW, unlabeled protein was blocked twice with 500 nmol of BG, and spleen was harvested for analysis. All animal experiments were approved by the "Service de la Consommation et des Affaires Vétérinaires du canton de Vaud."

SUPPLEMENTAL INFORMATION

Supplemental Information includes five figures, one table, and Supplemental Experimental Procedures and can be found with this article online at doi:10.1016/j.chembiol.2011.03.014.

ACKNOWLEDGMENTS

We thank Sujana Nylakonda, Christopher Towne, and Alexandra Quazzola for technical assistance, Johan Jakobsson and Andrea Corsinotti for KAP1 KO MEFs, Anna Groner for wt KAP1 vector, Pierre Maillard for sqTRIM5α plasmid, and all members of the Johnsson and Trono labs for discussions. This work was supported by the Swiss National Science Foundation, the Federal Office for Professional Education and Technology (CTI grant 8440), and the Fondation Claude et Giuliana. K.J. is a cofounder of Covalys Biosciences, which uses SNAP-tag for protein labeling.

Received: November 4, 2010
Revised: February 2, 2011
Accepted: March 8, 2011
Published: June 23, 2011

REFERENCES

Aiken, C., Konner, J., Landau, N.R., Lenburg, M.E., and Trono, D. (1994). Nef induces CD4 endocytosis: requirement for a critical dileucine motif in the membrane-proximal CD4 cytoplasmic domain. Cell *76*, 853–864.

Barde, I., Laurenti, E., Verp, S., Groner, A.C., Towne, C., Padrun, V., Aebischer, P., Trumpp, A., and Trono, D. (2009). Regulation of episomal gene expression by KRAB/KAP1-mediated histone modifications. J. Virol. *83*, 5574–5580.

Bateman, R.J., Munsell, L.Y., Morris, J.C., Swarm, R., Yarasheski, K.E., and Holtzman, D.M. (2006). Human amyloid-beta synthesis and clearance rates as measured in cerebrospinal fluid in vivo. Nat. Med. *12*, 856–861.

Bedford, L., Lowe, J., Dick, L.R., Mayer, R.J., and Brownell, J.E. (2011). Ubiquitin-like protein conjugation and the ubiquitin-proteasome system as drug targets. Nat. Rev. Drug Discov. *10*, 29–46.

Bremer, C., Tung, C.H., and Weissleder, R. (2001). In vivo molecular target assessment of matrix metalloproteinase inhibition. Nat. Med. *7*, 743–748.

Ciechanover, A. (2005). Proteolysis: from the lysosome to ubiquitin and the proteasome. Nat. Rev. Mol. Cell Biol. *6*, 79–87.

Dalgleish, A.G., Beverley, P.C., Clapham, P.R., Crawford, D.H., Greaves, M.F., and Weiss, R.A. (1984). The CD4 (T4) antigen is an essential component of the receptor for the AIDS retrovirus. Nature *312*, 763–767.

Daniels, D.S., Mol, C.D., Arvai, A.S., Kanugula, S., Pegg, A.E., and Tainer, J.A. (2000). Active and alkylated human AGT structures: a novel zinc site, inhibitor and extrahelical base binding. EMBO J. *19*, 1719–1730.

Dickson, R.C., and Mendenhall, M.D. (2004). Signal Transduction Protocols, *Volume 284*, 2nd edition (Totowa, NJ: Humana Press).

Dolan, M.E., Chae, M.Y., Pegg, A.E., Mullen, J.H., Friedman, H.S., and Moschel, R.C. (1994). Metabolism of O6-benzylguanine, an inactivator of O6-alkylguanine-DNA alkyltransferase. Cancer Res. *54*, 5123–5130.

Fernandez-Suarez, M., and Ting, A.Y. (2008). Fluorescent probes for super-resolution imaging in living cells. Nat. Rev. Mol. Cell Biol. *9*, 929–943.

Fuchs, J., Bohme, S., Oswald, F., Hedde, P.N., Krause, M., Wiedenmann, J., and Nienhaus, G.U. (2010). A photoactivatable marker protein for pulse-chase imaging with superresolution. Nat. Methods *7*, 627–630.

Gaietta, G., Deerinck, T.J., Adams, S.R., Bouwer, J., Tour, O., Laird, D.W., Sosinsky, G.E., Tsien, R.Y., and Ellisman, M.H. (2002). Multicolor and electron microscopic imaging of connexin trafficking. Science *296*, 503–507.

Giepmans, B.N., Adams, S.R., Ellisman, M.H., and Tsien, R.Y. (2006). The fluorescent toolbox for assessing protein location and function. Science *312*, 217–224.

Gronemeyer, T., Chidley, C., Juillerat, A., Heinis, C., and Johnsson, K. (2006). Directed evolution of O6-alkylguanine-DNA alkyltransferase for applications in protein labeling. Protein Eng. Des. Sel. *19*, 309–316.

Hein, B., Willig, K.I., Wurm, C.A., Westphal, V., Jakobs, S., and Hell, S.W. (2010). Stimulated emission depletion nanoscopy of living cells using SNAP-tag fusion proteins. Biophys. J. *98*, 158–163.

Hershko, A., and Ciechanover, A. (1998). The ubiquitin system. Annu. Rev. Biochem. *67*, 425–479.

Jansen, L.E., Black, B.E., Foltz, D.R., and Cleveland, D.W. (2007). Propagation of centromeric chromatin requires exit from mitosis. J. Cell Biol. *176*, 795–805.

Johnsson, N., and Johnsson, K. (2003). A fusion of disciplines: chemical approaches to exploit fusion proteins for functional genomics. ChemBioChem *4*, 803–810.

Keppler, A., Gendreizig, S., Gronemeyer, T., Pick, H., Vogel, H., and Johnsson, K. (2003). A general method for the covalent labeling of fusion proteins with small molecules *in vivo*. Nat. Biotechnol. *21*, 86–89.

Keppler, A., Pick, H., Arrivoli, C., Vogel, H., and Johnsson, K. (2004). Labeling of fusion proteins with synthetic fluorophores in live cells. Proc. Natl. Acad. Sci. USA *101*, 9955–9959.

Klein, T., Löschberger, A., Proppert, S., Wolter, S., van de Linde, S., and Sauer, M. (2011). Live-cell dSTORM with SNAP-tag fusion proteins. Nat. Methods *8*, 7–9.

Kreklau, E.L., Liu, N., Li, Z., Cornetta, K., and Erickson, L.C. (2001). Comparison of single- versus double-bolus treatments of O(6)-benzylguanine for depletion of O(6)-methylguanine DNA methyltransferase (MGMT) activity *in vivo*: development of a novel fluorometric oligonucleotide assay for measurement of MGMT activity. J. Pharmacol. Exp. Ther. *297*, 524–530.

Lakin, N.D., and Jackson, S.P. (1999). Regulation of p53 in response to DNA damage. Oncogene *18*, 7644–7655.

Lois, C., Hong, E.J., Pease, S., Brown, E.J., and Baltimore, D. (2002). Germline transmission and tissue-specific expression of transgenes delivered by lentiviral vectors. Science *295*, 868–872.

Mangasarian, A., Foti, M., Aiken, C., Chin, D., Carpentier, J.L., and Trono, D. (1997). The HIV-1 Nef protein acts as a connector with sorting pathways in the Golgi and at the plasma membrane. Immunity *6*, 67–77.

Marks, K.M., and Nolan, G.P. (2006). Chemical labeling strategies for cell biology. Nat. Methods *3*, 591–596.

Maurel, D., Comps-Agrar, L., Brock, C., Rives, M.L., Bourrier, E., Ayoub, M.A., Bazin, H., Tinel, N., Durroux, T., Prezeau, L., et al. (2008). Cell-surface protein-protein interaction analysis with time-resolved FRET and snap-tag technologies: application to GPCR oligomerization. Nat. Methods *5*, 561–567.

Maurice, M., Verhoeyen, E., Salmon, P., Trono, D., Russell, S.J., and Cosset, F.L. (2002). Efficient gene transfer into human primary blood lymphocytes by surface-engineered lentiviral vectors that display a T cell-activating polypeptide. Blood *99*, 2342–2350.

Mawuenyega, K.G., Sigurdson, W., Ovod, V., Munsell, L., Kasten, T., Morris, J.C., Yarasheski, K.E., and Bateman, R.J. (2010). Decreased clearance of CNS β-amyloid in Alzheimer's disease. Science *330*, 1774.

Pelchen-Matthews, A., Armes, J.E., Griffiths, G., and Marsh, M. (1991). Differential endocytosis of CD4 in lymphocytic and nonlymphocytic cells. J. Exp. Med. *173*, 575–587.

Pelchen-Matthews, A., Parsons, I.J., and Marsh, M. (1993). Phorbol ester-induced downregulation of CD4 is a multistep process involving dissociation from p56lck, increased association with clathrin-coated pits, and altered endosomal sorting. J. Exp. Med. *178*, 1209–1222.

Pham, W., Zhao, B.Q., Lo, E.H., Medarova, Z., Rosen, B., and Moore, A. (2005). Crossing the blood-brain barrier: a potential application of myristoylated polyarginine for *in vivo* neuroimaging. Neuroimage *28*, 287–292.

Quinn, J.A., Jiang, S.X., Reardon, D.A., Desjardins, A., Vredenburgh, J.J., Rich, J.N., Gururangan, S., Friedman, A.H., Bigner, D.D., Sampson, J.H., et al. (2009). Phase II trial of temozolomide plus o6-benzylguanine in adults with recurrent, temozolomide-resistant malignant glioma. J. Clin. Oncol. *27*, 1262–1267.

Ruegg, C.L., Rajasekar, S., Stein, B.S., and Engleman, E.G. (1992). Degradation of CD4 following phorbol-induced internalization in human T lymphocytes. Evidence for distinct endocytic routing of CD4 and CD3. J. Biol. Chem. *267*, 18837–18843.

Sabharwal, A., and Middleton, M.R. (2006). Exploiting the role of O6-methylguanine-DNA-methyltransferase (MGMT) in cancer therapy. Curr. Opin. Pharmacol. *6*, 355–363.

Salmon, P., and Trono, D. (2006). Production and titration of lentiviral vectors. Curr. Protoc. Neurosci., *Chapter 4*, Unit 4 21.

Shin, J.H., Ko, H.S., Kang, H., Lee, Y., Lee, Y.I., Pletinkova, O., Troconso, J.C., Dawson, V.L., and Dawson, T.M. (2011). PARIS (ZNF746) repression of

PGC-1alpha contributes to neurodegeneration in Parkinson's disease. Cell *144*, 689–702.

Shu, X., Royant, A., Lin, M.Z., Aguilera, T.A., Lev-Ram, V., Steinbach, P.A., and Tsien, R.Y. (2009). Mammalian expression of infrared fluorescent proteins engineered from a bacterial phytochrome. Science *324*, 804–807.

Sripathy, S.P., Stevens, J., and Schultz, D.C. (2006). The KAP1 corepressor functions to coordinate the assembly of de novo HP1-demarcated microenvironments of heterochromatin required for KRAB zinc finger protein-mediated transcriptional repression. Mol. Cell. Biol. *26*, 8623–8638.

Tannous, B.A., Grimm, J., Perry, K.F., Chen, J.W., Weissleder, R., and Breakefield, X.O. (2006). Metabolic biotinylation of cell surface receptors for *in vivo* imaging. Nat. Methods *3*, 391–396.

Tsukiji, S., Miyagawa, M., Takaoka, Y., Tamura, T., and Hamachi, I. (2009). Ligand-directed tosyl chemistry for protein labeling *in vivo*. Nat. Chem. Biol. *5*, 341–343.

Vivero-Pol, L., George, N., Krumm, H., Johnsson, K., and Johnsson, N. (2005). Multicolor imaging of cell surface proteins. J. Am. Chem. Soc. *127*, 12770–12771.

Xu-Welliver, M., and Pegg, A.E. (2002). Degradation of the alkylated form of the DNA repair protein, O(6)-alkylguanine-DNA alkyltransferase. Carcinogenesis *23*, 823–830.

Yen, H.C., Xu, Q., Chou, D.M., Zhao, Z., and Elledge, S.J. (2008). Global protein stability profiling in mammalian cells. Science *322*, 918–923.

